THE JOURNAL OF BIOLOGICAL CHEMISTRY
Vol. 274, No. 47, Issue of November 19, pp. 33565–33570, 1999

Printed in U.S.A.

Site-directed Mutagenesis of Cytochrome c_6 from *Anabaena* Species PCC 7119

IDENTIFICATION OF SURFACE RESIDUES OF THE HEMEPROTEIN INVOLVED IN PHOTOSYSTEM I REDUCTION*

(Received for publication, June 21, 1999, and in revised form, September 3, 1999)

Fernando P. Molina-Heredia, Antonio Díaz-Quintana, Manuel Hervás, José A. Navarro, and Miguel A. De la Rosa‡

From the Instituto de Bioquímica Vegetal y Fotosíntesis, Universidad de Sevilla y Consejo Superior de Investigaciones Científicas, Centro Isla de la Cartuja, Américo Vespucio s/n, 41092 Sevilla, Spain

A number of surface residues of cytochrome c_6 from the cyanobacterium *Anabaena* sp. PCC 7119 have been modified by site-directed mutagenesis. Changes were made in six amino acids, two near the heme group (Val-25 and Lys-29) and four in the positively charged patch (Lys-62, Arg-64, Lys-66, and Asp-72). The reactivity of mutants toward the membrane-anchored complex photosystem I was analyzed by laser flash absorption spectroscopy. The experimental results indicate that cytochrome c_6 possesses two areas involved in the redox interaction with photosystem I: 1) a positively charged patch that may drive its electrostatic attractive movement toward photosystem I to form a transient complex and 2) a hydrophobic region at the edge of the heme pocket that may provide the contact surface for the transfer of electrons to P_{700}. The isofunctionality of these two areas with those found in plastocyanin (which acts as an alternative electron carrier playing the same role as cytochrome c_6) are evident.

In cyanobacteria and green algae, cytochrome (Cyt)[1] c_6 acts as a soluble redox carrier that can replace plastocyanin in the transport of electrons between the two membrane-embedded complexes Cyt b_6f and photosystem I (PSI) (see Refs. 1 and 2 for reviews). In higher plants, however, the copper protein is the only electron carrier. The cyanobacterium *Anabaena*, like some other organisms, is able to synthesize either Cyt c_6 or plastocyanin (which both exhibit a basic isoelectric point of ~9) as a function of copper concentration in the growing medium (3).

The structures and functions of these two metalloproteins have been extensively studied in a wide range of organisms (4–11). According to our laser flash-induced kinetic studies, the reaction mechanism of PSI reduction follows three different models: type I, which involves an oriented collision between the two redox partners; type II, which proceeds through the formation of a transient complex prior to electron transfer; and type III, which requires an additional rearrangement step so as to make the redox centers orientate properly within the complex (9). During the evolution of photosynthetic organisms, interaction between a positively charged Cyt c_6 and PSI was first optimized (as is the case with *Anabaena* Cyt c_6, which follows the type III mechanism) and only later in evolution was a more complex kinetic mechanism developed with plastocyanin (2).

The three-dimensional structures of Cyt c_6 from the two eukaryotic green algae *Monoraphidium* (12) and *Chlamydomonas* (13) and from the cyanobacterium *Synechococcus* (14) have been solved. The analysis of the Cyt c_6 molecule compared with the plastocyanin structure allowed us to identify a hydrophobic region around the solvent-exposed heme propionates that resembles the north pole of plastocyanin as well as a negatively charged patch in eukaryotic Cyt c_6 similar to the east face of eukaryotic plastocyanin (12). In *Anabaena*, neither Cyt c_6 nor plastocyanin exhibits the acidic patches at their east face, which is rather positively charged (2).

Extensive mutagenesis studies of plastocyanin have supplied relevant information on the role of specific residues located both in its north and east faces (5, 8, 15–17). Recently, we performed a site-directed mutagenesis analysis of *Synechocystis* Cyt c_6 (18). Aspartates 70 and 72 appear to be located in a negatively charged region of Cyt c_6 that may be isofunctional with the well known "south-east" acidic patch of plastocyanin. In addition, Phe-64 (which is close to the heme group and could be the counterpart of Tyr-83 in plastocyanin (19)) does not appear to be involved in the electron transfer to PSI. In contrast, Arg-67, which is located at the edge of the Cyt c_6 acidic area, seems to be crucial.

This paper reports the kinetic and thermodynamic characterization of PSI reduction by a set of site-directed mutants of *Anabaena* Cyt c_6. The results demonstrate that a single mutation of specific residues in the hydrophobic or positively charged area of Cyt c_6 can promote drastic changes in the reaction mechanism. The two functional areas of Cyt c_6 involved in PSI photoreduction have been identified.

EXPERIMENTAL PROCEDURES

Purification of Native Cytochrome c_6—The hemeprotein from *Anabaena* sp. PCC 7119 was purified as described previously (11), but with slight modifications. Cyt c_6 samples were applied to a CM-cellulose column after oxidation with potassium ferricyanide. Elution of the adsorbed proteins was performed with a 50 μM potassium ferricyanide solution in a linear gradient of 2–30 mM potassium phosphate buffer, pH 7.0. The fractions containing pure Cyt c_6 were pooled, concentrated on an Amicon pressure-dialysis cell fitted with a YM-10 membrane, and stored at −80 °C. Cyt c_6 concentration was determined spectrophotometrically using an absorption coefficient of 26.2 mM^{-1} cm^{-1} at 553 nm for the reduced protein (20).

Construction of Mutants—The mutant *petJ* genes were constructed by polymerase chain reaction with the QuickChange kit (Stratagene)

* This work was supported by Dirección General de Investigación Científica y Técnica Grant PB96–1381, European Union Grant ERB-FMRX-CT98-0218, and Junta de Andalucía Grant CVI-0198. The costs of publication of this article were defrayed in part by the payment of page charges. This article must therefore be hereby marked "*advertisement*" in accordance with 18 U.S.C. Section 1734 solely to indicate this fact.

‡ To whom correspondence should be addressed. Tel.: 34-954-489506; Fax: 34-954-460065; E-mail: marosa@cica.es.

[1] The abbreviations used are: Cyt, cytochrome; PSI, photosystem I; Tricine, *N*-[2-hydroxy-1,1-bis(hydroxymethyl)ethyl]glycine; WT, wild-type; k_{bim}, bimolecular rate constant for the overall reaction; k_{inf}, diffusion-limited rate constant.

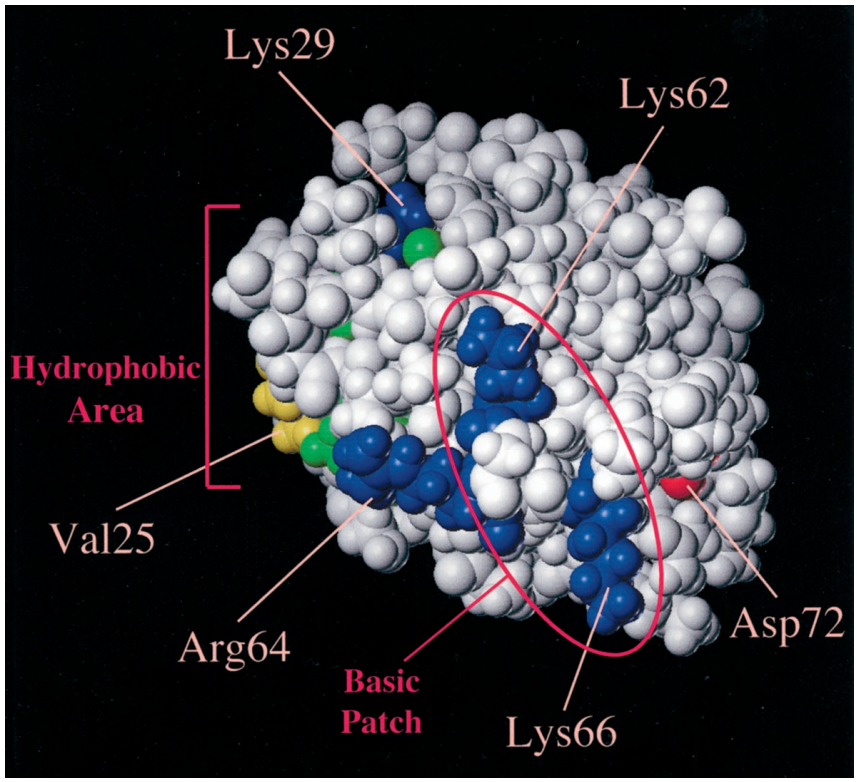

FIG. 1. **Space-filling model of cytochrome c_6 showing the residues modified by mutagenesis.** The molecule is oriented to show the six residues mutated; the "east" positively charged patch (equivalent to the acid face of eukaryotic cytochrome c_6 and plastocyanin) is in front, whereas the "north" hydrophobic patch is on the left. The heme group is depicted in *green*.

using oligonucleotides of 32 base pairs, 15 ng of DNA templates, and 12 min of extension time. The previously described expression construction for the *petJ* gene from *Anabaena* (21) was used as a template. The DNA sequencing service MediGenomix carried out the nucleotide sequence analysis. Other molecular biology protocols were standard (22).

Production of Recombinant Proteins and Purification Procedures—*Escherichia coli* MC1061-transformed cells were grown in M9 medium (22) supplemented with 1 g/liter Tryptone, 6 mg/liter Fe(III) ammonium citrate, and 100 μg/ml ampicillin. Cells from 10-liter microaerobic cultures were collected, and the periplasmic fraction was extracted according to the method of Hoshino and Kageyama (23) as modified by Eftekhar and Schiller (24). The resulting suspension was extensively dialyzed against 2 mM potassium phosphate, pH 7.0. From this point, the purification procedure was that for native Cyt c_6 (see above), with the exception of mutants K66E and D72K, which were eluted with buffer gradients ranging from 1 to 10 mM and from 2 to 120 mM, respectively. In all cases, 50 μM potassium ferricyanide was added to the gradient solutions to keep Cyt c_6 oxidized. Protein concentration was determined as described previously (21).

Redox Titrations—The redox potential value for the heme group in each Cyt c_6 mutant was determined as reported previously (21, 25), for which the differential absorbance changes at 553 *minus* 570 nm were followed. Errors in the experimental determinations were less than $\pm$5 mV.

Preparation of PSI Particles—PSI particles were isolated from *Anabaena* cells by β-dodecyl maltoside solubilization (26, 27). The chlorophyll/P_{700} ratio of the resulting PSI preparations was 140:1. The P_{700} content in PSI samples was calculated from the photoinduced absorbance changes at 820 nm using the absorption coefficient of 6.5 mM^{-1} cm^{-1} determined by Mathis and Sétif (28). Chlorophyll concentration was determined according to Arnon (29).

Laser Flash Absorption Spectroscopy—The kinetics of flash-induced absorbance changes in PSI were followed at 820 nm as described previously (9, 18). Experimental conditions and the standard reaction mixture were also as reported previously (17); the buffer used throughout this work was 20 mM Tricine/KOH, pH 7.5. Unless otherwise indicated, low and high ionic strengths refer to the absence and addition of 10 mM $MgCl_2$, respectively. Data collection and kinetic and thermodynamic analyses were carried out as reported by Hervás *et al.* (9, 10). Apparent thermodynamic parameters were estimated as described Díaz *et al.* (6) by fitting the experimental data to the Watkins equation (30). The values for the rate constant for electron transfer and K_A (see below) were determined according to the formalism by Meyer *et al.* (31).

Structure Simulation—The structures of WT and mutant Cyt c_6 were modeled using the SYBYL program (Tripos Associates) in an SGI RC10000 workstation. The three-dimensional crystal structure of Cyt c_6 from the green alga *Monoraphidium braunii* (12) was used as a template. Sequence alignment and subsequent amino acid substitution were performed with the BIOPOLYMER module of SYBYL Version 6.4. Force field parameters for the heme moiety were those in the AMBER package (32). The resulting file was first submitted to energy minimization *in vacuo* up to a root mean square energy gradient of 0.41 kJ mol^{-1} $Å^{-1}$ using the SANDER module of AMBER Version 4.1 (33). During these calculations, the backbone heavy atoms of α-helix regions were restrained at their position by a harmonic force of 62.7 kJ mol^{-1} $Å^{-1}$. Then, the whole system was solvated with three-point water molecules using the BLOB option of the EDIT module. Solvent was energy-minimized and submitted to a 9-ps molecular dynamics calculation. The whole system was again energy-minimized and submitted to a 1250-ps molecular dynamics run at 300 K. A total of 10 samples from the last 400 ps of trajectory were quenched by freezing the system in six steps of 1.5 ps. The qualities of the resulting structures were tested using the PROCHECK program (34). Surface electrostatic potentials were estimated using the algorithm of Nicholls and Honig (35), as indicated in the MOLMOL program (36).

RESULTS

To analyze the role of specific residues of *Anabaena* Cyt c_6 in the reaction mechanism of PSI reduction, six amino acids (two near the heme group and four in the positively charged east face) were chosen for mutations (Fig. 1). At the edge of the heme crevice, modifications were made at residues 25 and 29: Val-25, which is located near the heme β-*meso*-position, was substituted by alanine and glutamate; and Lys-29, which exhibits its side chain lying close to propionate 7, was replaced with histidine. Val-25 is located in the middle of the hydrophobic patch, but Lys-29 is not. However, mutation of the latter to histidine was considered to be interesting because the residue at position 29 is lysine in all Cyts c_6 with the exception of that from *Monoraphidium*, in which it is histidine (actually, the EPR spectra of *Monoraphidium* Cyt c_6 suggested an unusual histidine-histidine axial coordination for the heme iron, a ligand system that is not possible in the rest of Cyts c_6 with just one histidine residue (37)). In addition, basic residues at positions 28–30 in type I cytochromes have been proposed to con-

TABLE I
Midpoint redox potential and kinetic characterization of WT and mutant cytochrome c_6

Cytochrome c_6	E_m, pH 7.5	k_{bim}	$k_{inf} \times 10^{-6}$	k_{et} [a] $\times 10^{-5}$	FP	Type of mechanism
	mV	$M^{-1} s^{-1}$	$M^{-1} s^{-1}$	s^{-1}	%	
WT	337	11.3×10^7	11.4	1.7	35	III
V25A	286	6.9×10^7	6.4			I
V25E	287	0.2×10^7	0.2			I
K29H	272	6.2×10^7	11.0			I
K62E	340	4.9×10^7	9.4			I
R64E	320	2.2×10^7	2.6			I
K66E	335	5.7×10^7	11.7			I
D72K	338	1.5×10^{3} [b]	11.2	1.5	30	II

[a] k_{et}, electron transfer rate constant; FP, fast phase.
[b] This value stands for the rate constant of association between D72K and PSI.

trol the redox potential of the heme group through stabilization of propionate 7 (38). On the east face, modifications included the replacement of Lys-62 and Lys-66 by glutamates; Asp-72, which is also located in the middle of the east patch, was changed to lysine. Finally, Arg-64, which is at the edge of the east patch and has been shown to be crucial in *Synechocystis* Cyt c_6 (18), was replaced with glutamate.

The EPR and electronic absorption spectra of *Anabaena* Cyt c_6 were not changed by the mutations (data not shown), but its midpoint redox potential (E_m) could be significantly affected (Table I). The E_m value was unchanged when the residue mutated was at the east face, including Arg-64, but it was ~50 mV lower when the mutations were located near the heme group. Only minor differences were observed in the ^{1}H NMR spectra and nuclear Overhauser effect intensities of heme resonances with protons from other residues.[2]

The kinetics of PSI reduction by WT Cyt c_6 are biphasic, but those with the mutants (with the exception of D72K) are monoexponential, lacking the fast phase typically observed with the WT species. As shown in Fig. 2, the kinetics corresponding to D72K and WT Cyt c_6 exhibited a sharp initial fast phase (with a rate constant that was independent of donor protein concentration) followed by a slower decay. In contrast, the oscilloscope traces with mutants V25A and V25E fit to single exponential curves.

Fig. 3 shows that the observed pseudo first-order rate constant (k_{obs}) of PSI reduction by any mutant (with the exception of D72K) varied linearly with Cyt c_6 concentration. This can be interpreted by assuming that there is no formation of any stable complex between PSI and Cyt c_6, and the reaction thus follows a collisional kinetic mechanism (type I). With mutant D72K, however, the protein concentration dependence of k_{obs} exhibited a saturation profile, which indicates the formation of a bimolecular Cyt c_6·PSI complex prior to electron transfer. The extrapolated rate constant at infinite D72K concentration is similar to its electron transfer rate constant, which is obtained directly from the fast kinetic phase, thus suggesting a type II mechanism.

Such a saturation profile with D72K was even more evident at lower ionic strengths, which increase attractive electrostatic interactions. As shown in Fig. 4, the D72K mutant showed efficient complex formation, with an equilibrium constant (K_A) of 1.06×10^5 M^{-1} at low ionic strength. Extrapolation of the observed rate constant to infinite D72K concentration yielded a value that approached one-half the experimental electron transfer rate constant, which indicates that this mutant may follow a type III mechanism at low ionic strength. This finding

[2] A. Díaz-Quintana, M. Hervás, J. A. Navarro, and M. A. De la Rosa, unpublished data.

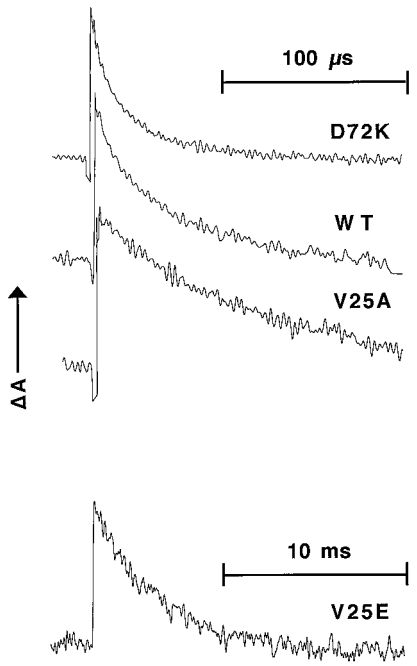

FIG. 2. **Kinetic traces showing PSI reduction by WT and mutant cytochrome c_6.** The hemeprotein concentration was 150 μM, and the pH value was 7.5. The oscilloscope traces obtained with the WT molecule and D72K fit to biphasic kinetics, whereas those corresponding to mutants V25A and V25E fit to single exponential curves.

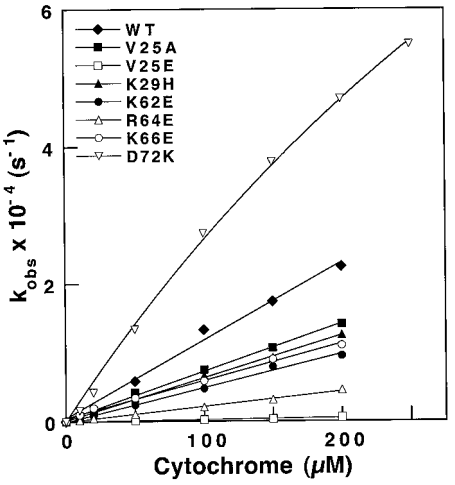

FIG. 3. **Dependence upon cytochrome c_6 concentration of k_{obs} for PSI reduction by the WT species and a set of mutants of the hemeprotein.** The *solid line* for mutant D72K corresponds to the theoretical fitting described by Meyer *et al*. (31). Experimental conditions were as described in the legend to Fig. 2.

also suggests that the rearrangement step (see above) is not limiting at high ionic strength.

Fig. 4 also shows that the V25A mutant was likewise able to form a transient complex with PSI at low ionic strength, even though its kinetic profiles of PSI reduction were monophasic at any ionic strength. The K_A value for complex formation between V25A and PSI is 1.07×10^4 M^{-1}, which is 10 times lower than that with D72K. These data indicate that V25A follows a type II mechanism in the absence of $MgCl_2$ and a type I mechanism when 10 mM $MgCl_2$ is added.

The bimolecular rate constant for the overall reaction (k_{bim}) of PSI reduction, which can be calculated from the linear plots in Fig. 3, is smaller with any mutant than with WT Cyt c_6 (Table I). In the hydrophobic patch, replacement of Val-25 with alanine or glutamate promoted a decrease in k_{bim} of ~2 and 60

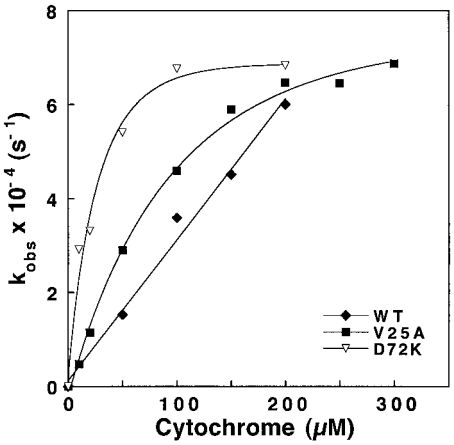

FIG. 4. **Dependence upon hemeprotein concentration of k_{obs} for PSI reduction by WT cytochrome c_6 and its mutants V25A and D72K at low ionic strength.** The *solid lines* for the mutants correspond to theoretical fittings according to Meyer *et al.* (31). The experimental conditions were as described in the legend to Fig. 2, except that magnesium chloride was omitted from the reaction mixture.

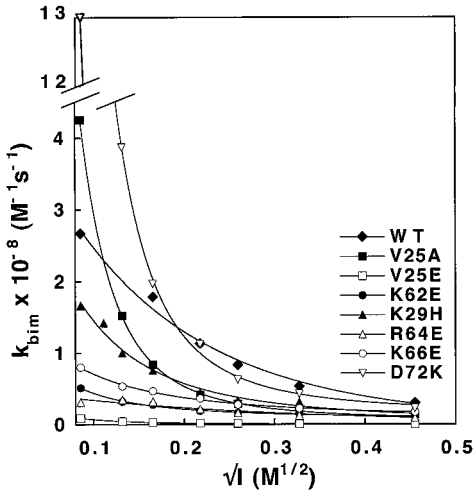

FIG. 5. **Effect of ionic strength on k_{bim} for PSI reduction by WT cytochrome c_6 and its mutants.** Experimental conditions were as described in the legend to Fig. 4, but the ionic strength was adjusted to the desired value by adding small amounts of a concentrated NaCl solution.

times, respectively, whereas mutation of Lys-29 to histidine involved a parallel decrease of ~50% as compared with WT Cyt c_6. Substitution of Arg-64, in its turn, by glutamate induced the rate constant to decrease by a factor of 5. In the east face, replacement of Lys-62 and Lys-66 with glutamate made the k_{bim} value decrease to half that of WT Cyt c_6. In the case of D72K, it should be noted that the bimolecular rate constant in Table I refers to its association constant, which is kinetically different from the other k_{bim} values in the table. Its electron transfer rate constant, calculated directly from the fast phase, compares well with that of WT Cyt c_6, as does the maximum percentage of fast phase (Table I).

Taking into account the electrostatic nature of the interaction of Cyt c_6 with PSI, a detailed analysis of the effect of ionic strength on k_{bim} was performed. Fig. 5 shows that the k_{bim} values with WT Cyt c_6 monotonically diminished with increasing NaCl concentration, thereby indicating the existence of attractive electrostatic interactions between the reaction partners as described previously (10, 11). A similar effect of ionic strength on k_{bim} was observed with all mutants, but some differences could be found among them. Actually, the k_{bim} values with mutants V25A and D72K are significantly higher than that with WT Cyt c_6 at low ionic strength, but they decreased drastically upon small additions of NaCl. Mutant K29H showed an ionic strength dependence similar to that of WT Cyt c_6, although its electron transfer efficiency was lower in the whole range analyzed. The k_{bim} values with all the other mutants are lower than that with WT Cyt c_6, indicating that the changes in net electrostatic charge alter the attractive interactions between PSI and mutant proteins.

Using the Watkins equation (30), the bimolecular rate constant extrapolated to infinite ionic strength (k_{inf}) (which facilitates the analysis of the intrinsic reactivity of redox partners in the absence of electrostatic interactions) can be calculated from the experimental data. As shown in Table I, the k_{inf} values with Cyt c_6 mutated at the positively charged patch are very similar to that with WT Cyt c_6, a fact that can be explained by assuming that the changes in reactivity induced by these mutations are mainly due to electrostatic, and not structural, effects. The only exception is R64E, for which the k_{inf} value is 4–5 times lower than that with WT Cyt c_6, a finding suggesting that the change in electrostatic charge is not the only factor affecting its reactivity toward PSI, as reported previously for *Synechocystis* Cyt c_6 (18). The effect of the K29H mutation seems to be merely electrostatic in nature, as k_{inf} is similar to that with WT Cyt c_6. The two mutations at position 25 involve modifications that make k_{inf} lower (the V25E mutant, in particular, exhibits a k_{inf} value that is 70 times lower than that with WT Cyt c_6).

To gain further insights into the nature of the interactions between PSI and Cyt c_6, a thermodynamic analysis of PSI reduction by the Cyt c_6 mutants was performed. In all cases, the temperature dependence of the observed rate constant (k_{obs}) yielded linear Eyring plots with no breakpoints, from which the values for the apparent activation enthalpy ($\Delta H^{\ddagger}$), entropy ($\Delta S^{\ddagger}$) and free energy ($\Delta G^{\ddagger}$) of the overall reaction could be calculated. For comparative purposes, Table II shows the differences in such activation parameters between WT Cyt c_6 and every mutant. The greatest difference was observed with V25E, whose free energy change is 9.41 kJ mol^{-1} higher than that of WT Cyt c_6, as expected from its inefficient interaction with PSI. This difference is due mainly to a decrease in the entropic term by ~28 J mol^{-1} K^{-1}. Also interesting is mutant R64E, whose free energy change is 4.15 kJ mol^{-1} higher than that of WT Cyt c_6, a fact that is due to changes in both the enthalpic and entropic terms. Mutant V25A behaved differently than any other mutant; in fact, the free energy term of its reaction is similar to that of WT Cyt c_6 despite the fact that both entropy and enthalpy show dramatic changes as compared with the thermodynamic parameters of WT Cyt c_6.

To check whether the differences in $\Delta G^{\ddagger}$ between WT and mutant Cyt c_6 ($\Delta\Delta G^{\ddagger}$) were due to electrostatic interactions, the experimental data were fitted to the Watkins equation (30). As shown in Fig. 6, the $\Delta\Delta G^{\ddagger}$ values with D72K and V25A perfectly fit the Watkins equation, and those of K29H, K62E, and K66E roughly fit it. Mutants V25E and R64E showed a linear NaCl dependence of $\Delta\Delta G^{\ddagger}$ at high ionic strength that caused the data to deviate from the Watkins equation.

DISCUSSION

Up to now, the only site-directed mutational analysis of any Cyt c_6 was recently reported by De la Cerda *et al.* (18) in the cyanobacterium *Synechocystis*. This hemeprotein, which is almost neutral, reacts with PSI according to a simple collisional model (type I). On the contrary, *Anabaena* Cyt c_6 is a positively charged protein that exhibits strong electrostatic attractions toward PSI (9, 11) and that reacts with the photosystem following a more complex three-step mechanism (type III). The

goal of this study was to elucidate the role played by some specific amino acids of *Anabaena* Cyt c_6 in such an attractive interaction with PSI and to investigate the possible involvement of its hydrophobic north area in the type III reaction mechanism.

TABLE II
Differences in the thermodynamic activation parameters of PSI reduction by the mutants of cytochrome c_6 compared with the wild-type molecule under standard conditions

Cytochrome c_6	$\Delta\Delta G^{\ddagger}$	$\Delta\Delta H^{\ddagger}$	$\Delta\Delta S^{\ddagger}$
	kJ mol^{-1}	*kJ mol^{-1}*	*J mol^{-1} K^{-1}*
V25A	1.11	−9.14	−34.57
V25E	9.41	1.08	−27.93
K29H	1.48	2.45	3.26
K62E	2.10	2.16	0.21
R64E	4.15	−1.72	−19.69
K66E	1.69	2.04	1.20
D72K	1.33[a]		

[a] This value stands for $\Delta\Delta G^{\ddagger}$ at infinite ionic strength.

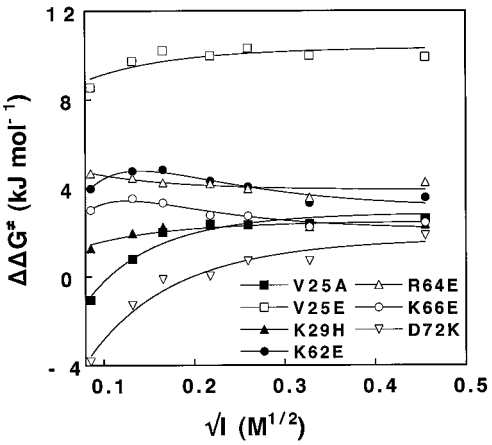

FIG. 6. **Effect of ionic strength on $\Delta\Delta G^{\ddagger}$ for PSI reduction by mutants of cytochrome c_6 as compared with the WT molecule.** Experimental conditions were as described in the legend to Fig. 5.

Mutations of Val-25 indicate that this residue may contribute to the specific topology of the north hydrophobic area of Cyt c_6 in its interaction with PSI. Similar conclusions were inferred from mutants at the north pole of eukaryotic plastocyanin (5, 8), in which the fast phase of electron transfer to PSI cannot be detected. This suggests that the mutant proteins (both Cyt c_6 and plastocyanin) are unable to reach the optimal orientation required for their redox centers to transfer electrons to PSI. It is interesting to compare the drastic effect induced by mutation of Val-25 to glutamate with mutation to alanine; the severe kinetic phenotype of V25E can be attributed to the presence of a negative charge in the middle of a normally hydrophobic region.

The K29H mutant possesses a redox potential value that is 65 mV more negative than that of WT Cyt c_6. This is probably due to the proximity of Lys-29 to heme propionate 7, in agreement with previous reports (38). Even though the driving force of electron transfer from K29H to PSI is higher, the kinetic profile of PSI reduction by the mutant loses the first fast phase, and its k_{bim} value is about half that of WT Cyt c_6. This can be ascribed in part to electrostatic effects, as the dependence of $\Delta\Delta G^{\ddagger}$ on ionic strength fits the Watkins equation (30), and the value for k_{inf} compares well with that of WT Cyt c_6. The change in redox potential induced by the mutation clearly does not affect reactivity with PSI, suggesting that complex formation is the rate-limiting step of the overall reaction.

Mutations of Lys-62 and Lys-66 at the positively charged patch of Cyt c_6 demonstrate that this region is responsible for the attractive electrostatic interactions with PSI. In *Anabaena*, the PsaF subunit does not seem to be directly involved in the interaction of PSI with its donor proteins, as is the case in *Synechocystis* (16, 39). Hence, the positive charges of *Anabaena* Cyt c_6 may interact with certain negatively charged areas in the PsaA/PsaB heterodimer of PSI to form a transient electrostatic complex. The surface electrostatic potential of WT and mutant Cyt c_6 was then calculated. Fig. 7 shows that the WT molecule has an extensive area of positive potential at its west face, *i.e.* close to the hydrophobic patch at the edge of the heme

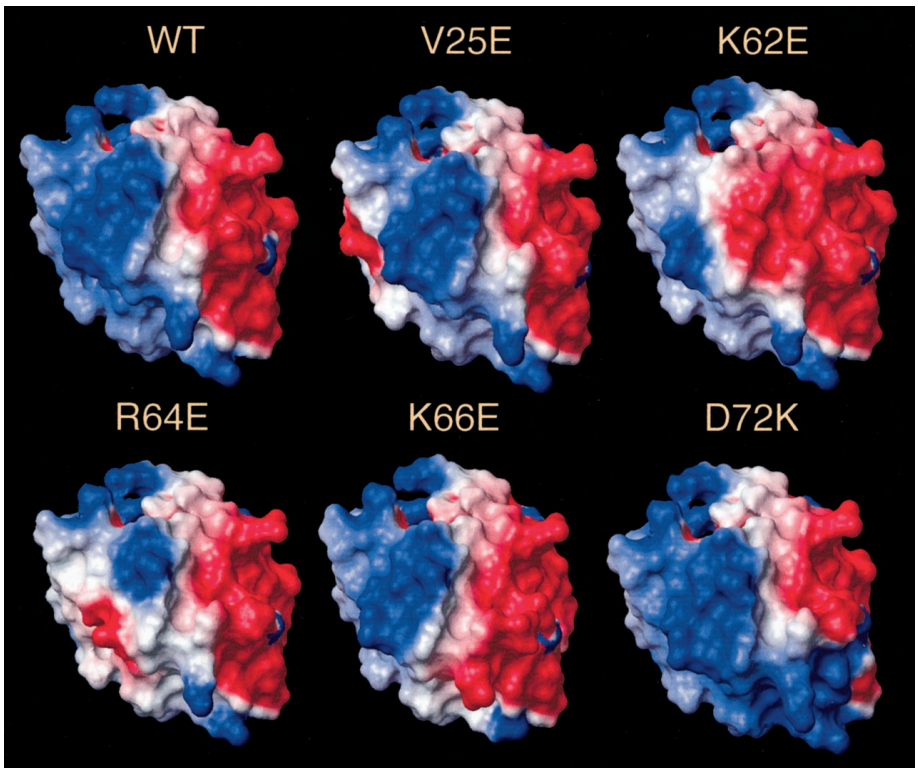

FIG. 7. **Distribution of the surface electrostatic potential of WT cytochrome c_6 and its mutants.** Electrostatic potential was calculated as indicated under "Experimental Procedures." Simulations were performed assuming an ionic strength of 40 mM at pH 7.0. Negative and positive potential regions are depicted in *red* and *blue*, respectively.

cleft. Mutants K66E, K62E, and R64E present a reduction in charge of the positive patch, although the change in the orientation of the dipole moment is <10°. This is consistent with the kinetic behavior exhibited by these three mutants, in which the ionic strength dependence of the interaction with PSI is not so much evident.

It is noteworthy that the effect of such mutations on the reaction rates can be closely correlated to changes in the positive electrostatic potential at the edge of the hydrophobic area. In fact, replacement of Arg-64 (which is located in the basic patch, adjacent to the hydrophobic region) by an acidic residue promotes a drastic reduction in size of the positive patch. Mutation of Lys-66 to glutamate likewise induces a diminution of the basic patch, but it does not alter the electrostatic surface potential at the edge of the hydrophobic area.

Mutant D72K is of special relevance as it clearly supports our proposal that the positively charged patch of Cyt c_6 is responsible for the interaction with PSI. Replacement of Asp-72 by a positive residue like lysine makes the positive potential region spread out (Fig. 7), thus favoring the attractive interactions with any negatively charged area of PSI. Like WT Cyt c_6, D72K is the only mutant that exhibits the fast kinetic phase of PSI reduction.

The thermodynamic analysis of PSI reduction by the mutants of Cyt c_6 revealed that all mutations induce changes in $\Delta H^{\ddagger}$ and $\Delta S^{\ddagger}$, but only some of them (V25A, V25E, and R64E) are significant. The large entropic changes of such mutants suggest that the solvent molecules are tuning the reactivity of the donor proteins toward PSI. The kinetic behavior of V25A indicates that the electrostatic interactions are predominant over hydrophobic forces.

To conclude, the experimental data reported here reveal that in *Anabaena* Cyt c_6, there are at least two interaction sites (which would be isofunctional with two similar areas in plastocyanin) for electron transfer to PSI: (i) a positively charged area, responsible for the electrostatic interactions forming the transient complex with the photosystem; and (ii) a hydrophobic region surrounding the heme pocket, responsible for the formation of the contact interphase with PSI allowing electrons to go from the heme iron to P_{700}^{+}. The main difference with respect to *Synechocystis* Cyt c_6 (18) is found at the electrostatically charged patch, which explains the differences in their respective reaction mechanisms of PSI photoreduction (10).

REFERENCES

1. Chitnis, P. R., Xu, Q., Chitnis, V. P., and Nechustai, R. (1995) *Photosynth. Res.* **44,** 23–40
2. Navarro, J. A., Hervás, M., and De la Rosa, M. A. (1997) *J. Biol. Inorg. Chem.* **2,** 11–22
3. Ho, K. K., and Krogmann, D. W. (1984) *Biochim. Biophys. Acta* **766,** 310–316
4. Bottin, H., and Mathis, P. (1985) *Biochemistry* **24,** 6453–6460
5. Sigfridsson, K., Young, S., and Hansson, Ö. (1996) *Biochemistry* **35,** 1249–1257
6. Díaz, A., Hervás, M., Navarro, J. A., De la Rosa, M. A., and Tollin, G. (1994) *Eur. J. Biochem.* **222,** 1001–1007
7. Drepper, F., Hippler, M., Nitschke, W., and Haehnel, W. (1996) *Biochemistry* **35,** 1282–1295
8. Haehnel, W., Jansen, T., Gause, K., Klösgen, R. B., Stahl, B., Michl, D., Huvermann, B., Karas, M., and Herrmann, R. G. (1994) *EMBO J.* **13,** 1028–1038
9. Hervás, M., Navarro, J. A., Díaz, A., Bottin, H., and De la Rosa, M. A. (1995) *Biochemistry* **34,** 11321–11326
10. Hervás, M., Navarro, J. A., Díaz, A., and De la Rosa, M. A. (1996) *Biochemistry* **35,** 2693–2698
11. Medina, M., Díaz, A., Hervás, M., Navarro, J. A., Gómez-Moreno, C., De la Rosa, M. A., and Tollin, G. (1993) *Eur. J. Biochem.* **213,** 1133–1138
12. Frazão, C., Soares, C. M., Carrondo, M. A., Pohl, E., Dauter, Z., Wilson, K. S., Hervás, M., Navarro, J. A., De la Rosa, M. A., and Sheldrick, G. (1995) *Structure* **3,** 1159–1169
13. Kerfeld, C. A., Anwar, H. P., Interrante, R., Merchant, S., and Yeates, T. O. (1995) *J. Mol. Biol.* **250,** 627–647
14. Beißinger, M., Sticht, H., Sutter, M., Ejchart, A., Haehnel, W., and Rösch, P. (1998) *EMBO J.* **17,** 27–36
15. Nordling, M., Sigfridsson, K., Young, S., Lundberg, L. G., and Hansson, Ö. (1991) *FEBS Lett.* **291,** 327–330
16. Hippler, M., Reichert, J., Sutter, M., Zak, E., Altschmied, L., Schröer, U., Herrmann, R. G., and Haehnel, W. (1996) *EMBO J.* **15,** 6374–6384
17. De la Cerda, B., Navarro, J. A., Hervás, M., and De la Rosa, M. A. (1997) *Biochemistry* **36,** 10125–10130
18. De la Cerda, B., Díaz-Quintana, A., Navarro, J. A., Hervás, M., and De la Rosa, M. A. (1999) *J. Biol. Chem.* **274,** 13292–13297
19. Ullmann, G. M., Hauswald, M., Jensen, A., Kostic, N. M., and Knapp, E.-W. (1997) *Biochemistry* **36,** 16187–16196
20. Medina, M., Louro, R. O., Gagnon, J., Peleato, M. L., Mendes, J., Gómez-Moreno, C., Xavier, A. V., and Teixeira, M. (1997) *J. Biol. Inorg. Chem.* **2,** 225–234
21. Molina-Heredia, F. P., Hervás, M., Navarro, J. A., and De la Rosa, M. A. (1998) *Biochem. Biophys. Res. Commun.* **243,** 302–306
22. Sambrook, J., Fritsch, E. F., and Maniatis, T. (1989) *Molecular Cloning: A Laboratory manual*, 2nd Ed., Cold Spring Harbor Laboratory, Cold Spring Harbor, NY
23. Hoshino, T., and Kageyama, M. (1980) *J. Bacteriol.* **141,** 1055–1063
24. Eftekhar, F., and Schiller, N. L. (1994) *Curr. Microbiol.* **29,** 37–42
25. Ortega, J. M., Hervás M., and Losada, M. (1988) *Eur. J. Biochem.* **199,** 239–243
26. Hervás, M., Ortega, J. M., Navarro, J. A., De la Rosa, M. A., and Bottin, H. (1994) *Biochim. Biophys. Acta* **1184,** 235–241
27. Rögner, M., Nixon, P. J., and Dinner, B. A. (1990) *J. Biol. Chem.* **265,** 6189–6196
28. Mathis, P., and Sétif, P. (1981) *Isr. J. Chem.* **21,** 316–320
29. Arnon, D. I. (1949) *Plant Physiol. (Bethesda)* **24,** 1–15
30. Watkins, J. A., Cusanovich, M. A., Meyer, T. E., and Tollin, G. (1994) *Protein Sci.* **3,** 2104–2114
31. Meyer, T. E., Zhao, Z. G., Cusanovich, M. A., and Tollin, G. (1993) *Biochemistry* **32,** 4552–4559
32. Giammona, D. A. (1984) *An Examination of Conformational Flexibility in Porphyrins and Bulky-ligand Binding in Myoglobin*. Ph.D. thesis, University of California, Davis, CA
33. Pearlman, D. A., Case, D. A., Cadwell, G. C., Siebel, G. L., Singh, U. C., Weiner, P., and Kollman, P. A. (1995) *AMBER Version 4.1.*, University of California, San Francisco
34. Laskowski, R. A., MacArthur, M. W., Moss, D. S., and Thornton, J. M. (1993) *J. Appl. Crystallogr.* **26,** 283–291
35. Nicholls, A., and Honig, B. (1991) *J. Comput. Chem.* **12,** 435–445
36. Koradi, R., Billeter, M., and Wuthrich, K. (1996) *J. Mol. Graph.* **14,** 51–55
37. Campos, A. P., Aguiar, A. P., Hervás, M., Regalla, M., Navarro, J. A., Ortega, J. M., Xavier, A. V., De la Rosa, M. A., and Teixeira, M. (1993) *Eur. J. Biochem.* **216,** 329–341
38. Moore, G., Harris, D. E., Leitch, F. A., and Pettigrew, G. W. (1984) *Biochim. Biophys. Acta* **764,** 331–342
39. Xu, Q., Chitnis, V. P., Yu, L., and Chitnis, P. R. (1994) *J. Biol. Chem.* **269,** 3205–3211